Advances in the light field displays based on integral imaging and holographic techniques

(Invited Paper)

Nam Kim*, Md. Ashraful Alam, Le Thanh Bang, Anh-Hoang Phan, Mei-Lan Piao, and Munkh-Uchral Erdenebat

School of Electrical and Computer Engineering, Chungbuk National University, 410 Sungbong-ro, Heungdeok-gu, Cheongju, Chungbuk 361-763, Korea

**Corresponding author: namkim@chungbuk.ac.kr*

Received March 4, 2014; accepted April 4, 2014; posted online May 20, 2014

Light field displays comprise three-dimensional (3D) visual information presentation devices capable of providing realistic and full parallax autostereoscopic images. In this letter, the recent advances in the light field displays based on integral imaging (II) and holographic techniques are presented. Several advanced approaches to demonstrate the light field displays including viewing angle enhancement techniques of the II display, a fast hologram generation method using graphics processing unit (GPU) and multiple WRPs, and a holographic microscopy to display the living cells are reported. These methods improve some important constraints of the light field displays and add new features.

OCIS codes: 100.6890, 110.0110, 090.0090.
doi: 10.3788/COL201412.060005.

Nowadays, a three-dimensional (3D) light field display has attracted a great deal of attention because of its attractive applications. By presenting a light field using technology that maps each sample to the appropriate ray in physical space, one obtains an autostereoscopic visual effect to observe the original scene. Several approaches have been developed[1−5] to demonstrate a light field display. In this letter, the recent advances in the light field displays using techniques, such as integral imaging (II), integral-floating display (IFD), holography, and holographic microscopy of live cell, are presented.

Among numerous light field displays, II is a powerful autostereoscopic 3D display technique that provides a number of attractive features such as full color, full-parallax 3D image with continuous viewpoints in normal room environment that distinguish the II from other techniques. Despite a number of attractive advantages, the II has some major drawbacks, such as limited resolution, narrow viewing angle, and small depth range, due to the specifications of the lens array. In all of the drawbacks of II, the narrow viewing angle is the most serious barrier to its commercial applications. Many researches have been conducted to overcome this problem[6], but II is still suffering for this limit. In order to develop a wide-viewing angled II display, a new approach to the viewing zone control of II display using a directional projection with a directional elemental image generation and resizing (DEIGR) algorithm, was successfully demonstrated and reported in a most recent study[7]. Using this method, the point light source (PLS)[8] of each elemental image (EI) shifts in terms of the projection angle, resulting in a shift in the viewing zone. The amount of viewing zone shifting has been formulized in terms of the projection angle. This method can control only the viewing zone of II display but it cannot widen the viewing angle itself. If multi-directional projections of a multiple sets of EIs are used with suitable projection angles in a sequential time-multiplex[9] manner, a wide-viewing-angled II display can be achieved. To implement a viewing angle enhanced II display system, a multi-directional projection scheme is proposed. Figure 1 illustrates the basic principle of the proposed method by using two-directional (2D) projections. In this method, each elemental lens of the lens array collects multi-directional illuminations of multiple EI sets and produces multiple PLSs at different positions in the focal plane; and the positions of the PLSs can be controlled by the projection angles. In this case, the viewing zone constitutes with multiple diverging ray bundles emerging from the multi-directional projections of multiple EI sets, which is wider than that of the conventional method; whereas the conventional system produces the

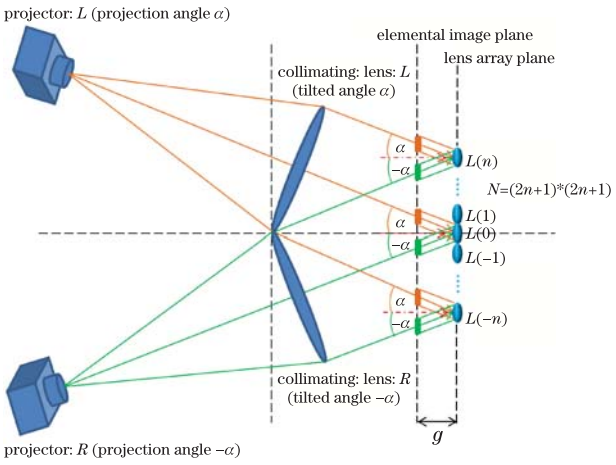

Fig. 1. (Color online) Principle of the viewing angle enhancement using multi-directional projections and DEIGR algorithm.

viewing zone using only a single set of EI projection. Hence the viewing angle of the reconstructed image is enhanced.

To verify the possibility of the viewing angle enhancement by using multi-directional EI projections with DEGIR algorithm[7], preliminary experiments using multi-directional (0°, 14°, and −14°) projections were conducted. Figure 2 shows the experimental results. Figure 2(a) presented the reconstructed 3D images for the 0° (central) projection viewed from the different viewing positions (left to rightmost positions). Figures 2(b) and (c) presented the reconstructed 3D images for 2D (14° and −14°) projections. From the Fig. 2(b), it is seen that the viewing zone is shifted by almost half of the total viewing angle as compared to the conventional method (as shown in Fig. 2(a)) due to the 14° directional EI projections. On the other hand, in the similar way: the viewing zone is shifted by the same amount to the opposite direction while projecting the EI with -14° directionally. As a result, the total viewing zone angles are enhanced by almost two-times wider than that of the conventional method as seen in the Fig. 2. Therefore, the reconstructed 3D images of Figs. 2(b) and (c) confirm that the 2D projection scheme is capable of enhancing the viewing angle of the proposed method almost two fold (see Figs. 2(b)−(c)) using the DEIGR algorithm. It can be noted that the reconstructed images in Figs. 2(b) and (c) were found with a 2D projection scheme but operated separately. By using 2D projections with a time-multiplex[9] sequential projection scheme, an enhanced viewing angle (which is almost two-times compared to the conventional method) can be found physically. In the further experiments, the time-multiplexed sequential projections scheme will be performed.

Another method to enhance the limited viewing angle of II display based on the spinning-mirror type volumetric light field display had been proposed[10]. The system

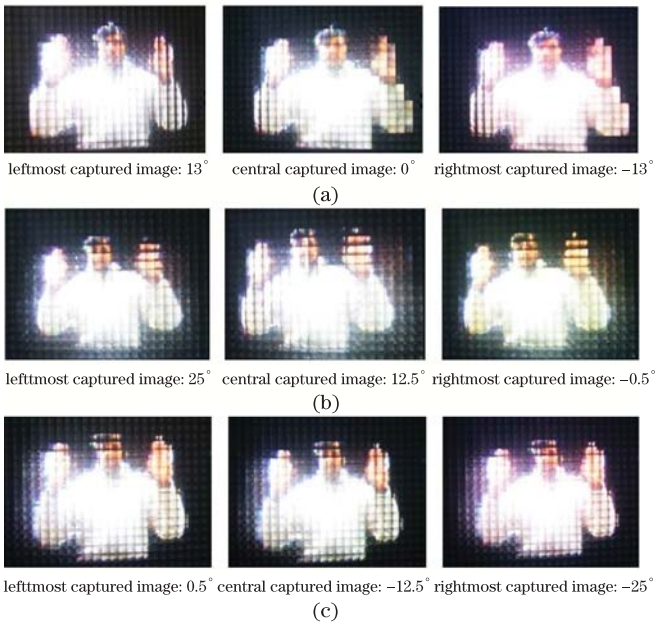

Fig. 2. (Color online) Reconstructed 3D images for multi-directional projections: (a) 0°, (b) 14° and (c) -14°, to verify the viewing angle enhancement using multi-directional projections.

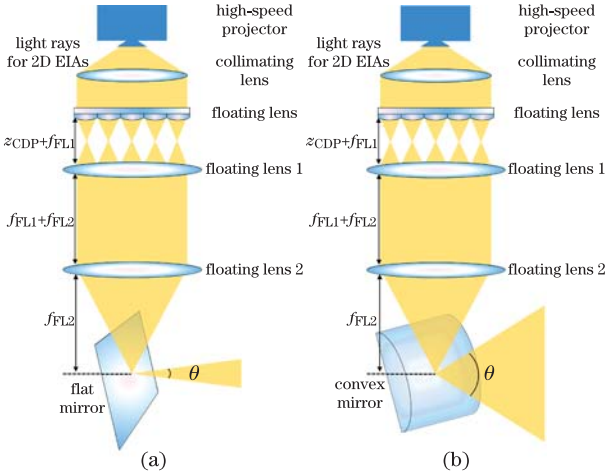

Fig. 3. (Color online) Basic structure of the 360° IFD: (a) conventional and (b) vertical viewing angle enhancement case.

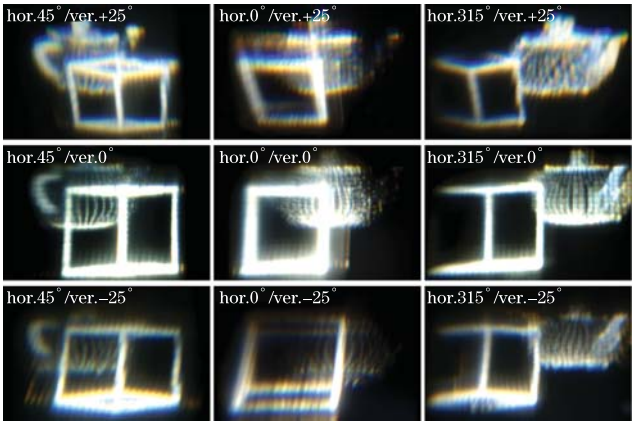

Fig. 4. (Color online) Experimental results, images captured from the multiple viewing directions: the center, the sides (45° and 315° each way), the top (+25°), and bottom (−25°).

consisted of a high-speed digital micromirror device (DMD) projector, a collimating lens, a lens array, double floating lenses, and a rotating mirror. Figure 3(a) shows the general configuration of the conventional 360° IFD. A lens array integrates the projected elemental image arrays (EIA) originated in the z_{CDP} and the reconstructed 3D perspectives are relayed on the center of the rotating mirror through double floating lenses with 4-f configuration. A high-speed motor rotates the mirror in synchronization with DMD projections. For the given mirror rotation angle, initial 3D perspectives in the lens array system are determined from all of the 3D object points displayed through the double floating lenses, and EIAs are generated for the initial 3D perspectives.

However, vertical viewing angle was very narrow. Owing to a function of the double floating lenses that decreases the viewing angle of initially reconstructed images to match them with the angular step of the mirror rotation and the reduced angle still remained intact in the final display. For the vertical viewing angle enhancement, vertically curved convex mirror is used instead of the flat mirror as shown in Fig. 3(b)[11]. The only difference of the mirror type shows large effectual results where the convex mirror disperses reflected light rays more widely in the vertical direction.

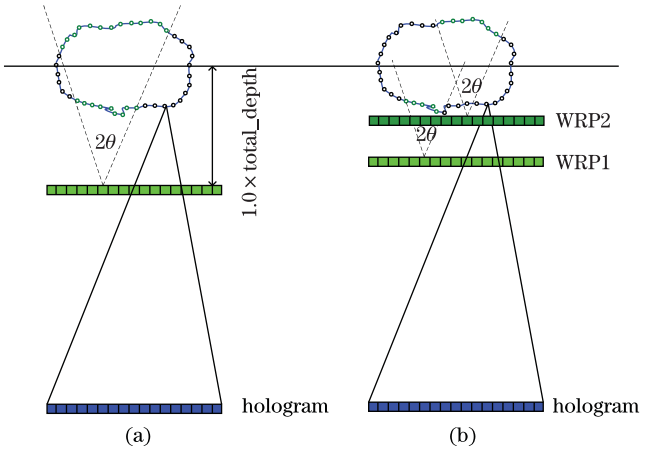

Fig. 5. (Color online) The scheme of wavefront recording method: (a) single WRP and (b) double WRPs.

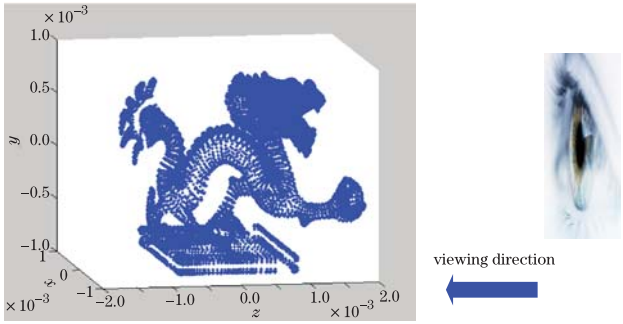

Fig. 6. (Color online) The "dragon" graphic object with 20k points having a depth of two times longer than the lateral size.

In the experiment, the natural full-parallax 3D image with enhanced vertical viewing angle in 360° viewing zone has been demonstrated successfully. Here, total 200 3D perspectives are relayed to the center of the mirror and a rotating mirror tailors the 3D perspectives in the horizontal direction where the mirror angular step is 1.8°. Convex mirror enhances the vertical viewing angle to approximately 50° where it was only 4-6° in the conventional 360° IFD. Figure 4 presents the experimental results. The displayed images are captured from center, sides (45° and 315° each way), and top and bottom views (taken from approximately ±25°).

In another study, a fast hologram generation method has been developed to reduce the calculation time and improve the quality of the reconstructed image as well, by using graphics processing unit (GPU) and multiple wavefront recording planes (WRP). The independency of capturing the optical field in hologram plane or emitting the field from object in pixels is the challenge to use the GPU to the parallel process. Therefore, the GPU can be used to capture the light field at a hologram or to emit the light from an object in a parallel process, where one thread controls the calculation for a single pixel. On the other hand, in this letter the WRP method is used to enhance the generation speed, which was first introduced by T. Shimobaba[12]. In this method, a virtual plane is placed near the object. The sampling pitch is dependent on the wavelength of illumination light and the recording angle (the angle between object beam and reference beam). So, the WRP plane is placed parallel to the hologram plane to prevent the violation of sampling theory. Firstly, the optical field from object to the computer generated hologram (CGH) plane is calculated on the virtual plane, and then the optical field in WRP is Fresnel transformed to the hologram plane by using fast Fourier transform (FFT). Using this method, the calculation time reduces because every object point is not calculated directly on hologram plane but on the WRP plane. The sampling pitch on WRP is kept the same as on the hologram plane. As the WRP plane is close to the object, so the active area of one object point is small according to the relation of recording distance, sampling pitch and recording area. Figure 5 shows the principle of the proposed WRP method. Each pixel in WRP plane only captures the light field from limited pixels of the object. In order to enhance the speed, we used multiple WRPs that reduced the active area so that it can reduce the time of calculation (Fig. 5(b)). The WRP plane cannot be placed very close to the object point. The WRP needs to be placed at a distance that is far enough to reduce the dynamic range of intensity. By analyzing the effect of WRP's position to maintain a good quality of the reconstruction of object, we choose a suitable position of placing the WRP far from the center of the object or the center of each section of the object (in case of multiple WRPs), which is equal to the total depth of the object. In multiple WRP method, the WRPs are placed at the distances that are equal to the depth of each section of the object as shown in Fig. 5(b).

The computer based experiment was performed to verify the idea. In this experiment, a graphic 3D model of a "dragon" with 20 k points was selected as an object, as shown in Fig. 6, and two WRPs were placed as configured in Fig. 5(b). The experiments were conducted on a Windows 7 64-bit operating system, MATLAB R2012b, Intel Xeon X5690@ 3.47 GHz CPU, and NVIDIA Tesla C2075 GPU. Table 1 lists the calculation time. The calculation time using double WRPs was considerably reduced compared with single WRP in both CPU and GPU.

The reconstruction of the object along with the z direction of multiple WRPs method is shown in Fig. 7.

Table 1. Calculation Time on the CPU and GPU for a Single WRP and that of the Proposed Method (in second)

	CPU	GPU
Single WRP	3804	0.177
Double WRP	2056	0.128

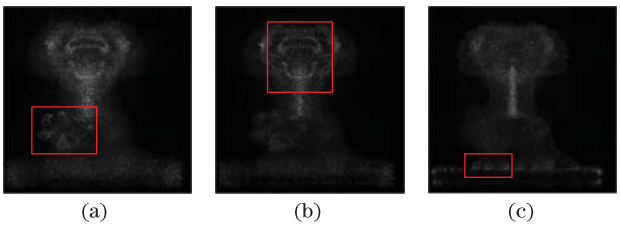

Fig. 7. (Color online) Reconstruction of dragon object with different depths: (a) focus to right-foreleg, (b) focus to head, and (c) focus to right-rearleg.

It can be seen in Fig. 7 that the reconstructed results have a good depth of focus (or depth of view). The right foreleg, head, and right rear leg were in focused area in Figs. 7(a), (b), and (c), sequentially. The focused areas have a high intensity point than the remaining area of the point cloud object as seen inside the red blocks in Fig. 7.

Reconstruction of 3D image of live cell usually uses laser microscopy as confocal and two-photon microscopy; this method has enabled high-resolution optical experiments in live samples. However, the laser microscopy is typically performed by sequentially scanning a single laser beam across a sample. Here, we report an optimized imaging system (i.e., holographic microscope), which integrates four phase-shifting hologram method and fluorescence cell method to have real 3D cell object. This method based on the emission wavelength from cell that dye fluorescence and a reference beam from a laser to calculate a hologram. From this, we can reconstruct real 3D cell. This method overcomes the disadvantage of laser microscopy that is the time of scanning and it provides enhanced resolution of 3D cell than the other method.

3D conventional light microscopes used in life sciences are based on the use of ultraviolet and visible radiation for optical analysis and microsurgery[13]. The diagnostic method include 3D confocal laser scanning fluorescence microscopy with excitation radiation of He-Ne lasers, argon/krypton ion lasers[14], He-Cd lasers, and laser diodes[15].

However, in the laser-scanning microscopes, the frame rate is intrinsically limited by two major factors. The first one is the physical response time of the scanners, typical galvanometer mirrors. The second, and more fundamental constraint on the overall speed of the system, is related to the physical processes of imaging.

The previous research overcomes this limit by using multi-beam scanning for allowing the increased speed and signal-to-noise ratio of the imaged samples, but was still limited by many of the problems that plague raster scanning, such as small dwell time for excitation per pixel. In these studies, to increase the speed and to solve the problems of the previous methods by using the advantage of holographic principles, we propose a method that can reduce the time needed to obtain a full information about the cell compared to the confocal microscopy method, and greater depth of resolution of the cell compared to the multi-photon fluorescence light microscopy method by combining the digital hologram method and the principle of multi-photon fluorescence light. In our proposed method, we need to generate a hologram from 3 to 10 layers for analysis, according to the holographic principle, and are able to reconstruct a cell with full depth of information. Therefore, the proposed method can reduce the time needed for scanning and increases the resolution of the cell. The principle of proposed method is shown in Fig. 8.

From the principles of photon cell and holography, the reconstruction of the 3D image of cell is implemented by the following steps:

First step: From four holograms recorded by the CCD by shifting holography, we have a complex hologram at a constant distance. This complex hologram is the hologram's plane of the cell that has the focal point of the object lens. Therefore, the hologram recorded in this case is a hologram of the object points on the plane's focal point or around this plane with a distance of $\Delta\eta$. The value of $\Delta\eta$ depends on the size of pin hole placed next to the objective lens. With the size of pin hole of 50 μm, $\Delta\eta$=2 μm is the best for the reconstructed object. It has been shown in Fig. 9. The excitation and emission spectra of green fluorescent protein (GFP), and the reconstructed 3D cell with phase-shifting hologram are shown in Figs. 9(a) and (b) respectively.

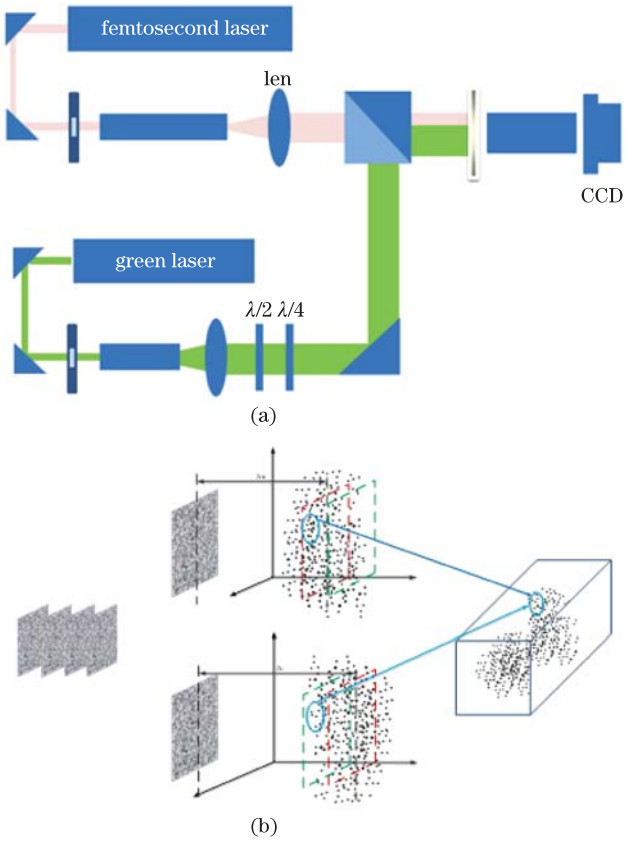

Fig. 8. (Color online) (a) Principle of the proposed method and (b) comparison of the object point between two layers.

Second step: For each complex hologram, we reconstructed a 3D object using the hologram principle and using reduced depth of focus by Wiener filter, to reduce noise and some object-point errors on each plane. The result is a whole object point on the plane that has a 2-μm thickness. Each thick plane of object points is actually a layer of the living cell, and by combining whole 3D layers and checking object points on the border of the layers and inside layers, we reconstruct a living cell including both the interior and the exterior of the cell.

In conclusion, we report some recent advances in the light field displays using several methods based on integral imaging and holographic techniques. The viewing angle enhancement method is introduced based on the multi-directional projections scheme, which can enhance the viewing angle depending on the directional projection angles and the number of elemental image sets used. In the integral-floating display presented in this letter, both the horizontal (360°) and vertical (±25°) viewing angle is enhanced, whereas the vertical viewing angle is very small (i.e., ±3°) in the previous method[10].

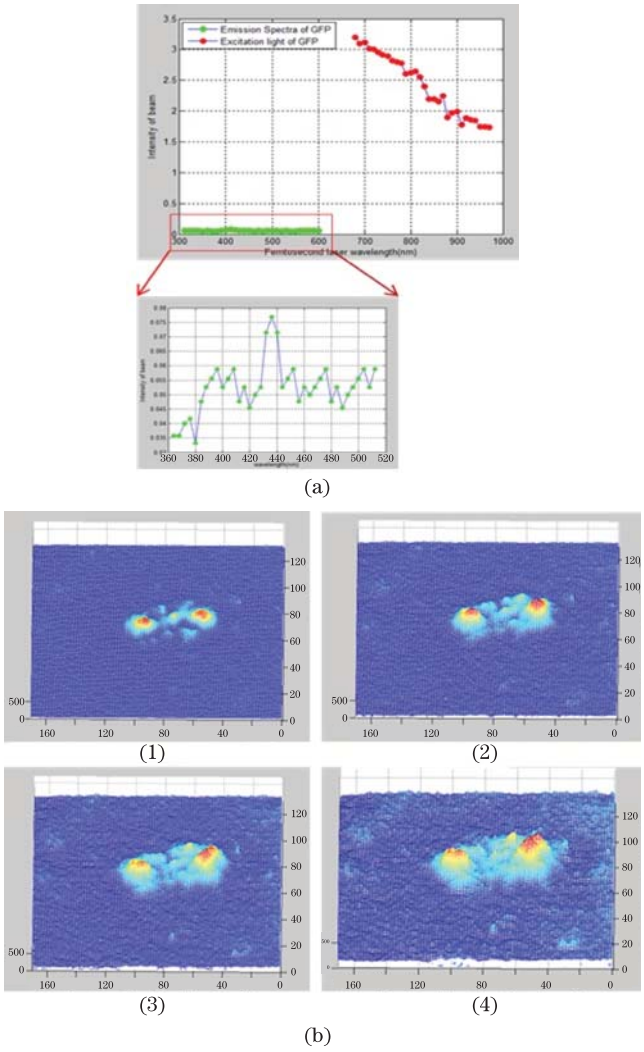

Fig. 9. (Color online) (a) Excitation and emission spectra of GFP (Green Fluorescent Protein) and (b) reconstructed 3D cell with phase-shifting hologram: (1) first layers (distance from CCD to first focus plane: 50 mm), (2) second layer (50 mm+2 μm ($\Delta\eta$)), (3) third layer (50 mm+4 μm ($\Delta\eta$)), and (4) combining these three layers.

Using the holographic technique, a fast hologram generation method is developed using multiple WRPs and GPU parallel processing that reduces the computation time for hologram generation. Another new approach to the holographic microscopy method is demonstrated to display a 3D image of live cells. It is verified by the experimental results, as shown in Fig. 9. This method overcomes the important constraints of the existing techniques, such as reduces the physical response time of scanning using a four-phase shifting hologram method and improves the image quality by decreasing the proximity.

This work was supported by the National Research Foundation of Korea (NRF) grant, funded by the Korea government (MSIP) (No. 2013-067321); and partly supported by the Korea Creative Content Agency (KOCCA) in the Culture Technology (CT) Research & Development Program 2013.

References

1. G. Wetzstein, D. Lanman, W. Heidrich, and R. Raskar, ACM Trans. Graph. **30,** 95 (2011).
2. D. Lanman, M. Hirsch, Y. Kim, and R. Raskar, ACM Trans. Graph. **29,** 163 (2010).
3. N.-Y. Jo, H.-G. Lim, S.-K. Lee, Y.-S. Kim, and J.-H. Park, Opt. Express **21,** 29628 (2013).
4. H.-S. Kim, K.-M. Jeong, S.-I. Hong, N.-Y. Jo, and J.-H. Park, Opt. Express **20,** 23755 (2012).
5. S. Park, B.-S. Song, and S.-W. Min, J. Opt. Soc. Korea **14,** 121 (2010).
6. J.-H. Park, K. Hong, and B. Lee, Appl. Opt. **48,** H77 (2009).
7. M. A. Alam, M.-L. Piao, L. T. Bang, and N. Kim, Appl. Opt. **52,** 6969 (2013).
8. Y. Kim, J. Kim, J.-M. Kang, J.-H. Jung, H. Choi, and B. Lee, Opt. Express **15,** 18253 (2007).
9. A. Stern and B. Javidi, Appl. Opt. **42,** 7036 (2003).
10. M.-U. Erdenebat, G. Baasantseren, N. Kim, K.-C. Kwon, J. Byeon, K.-H. Yoo, and J.-H. Park, J. Opt. Soc. Korea **16,** 365 (2012).
11. M.-U. Erdenebat, G. Baasantseren, J.-H. Park, N. Kim, K.-C. Kwon, Y.-H. Jang, and K.-H. Yoo, Proc. SPIE **7863,** 7863OU (2011).
12. T. Shimobaba, N. Masuda, and T. Ito, Opt. Lett. **34,** 3133 (2009).
13. K. König, S Simon, and K.-J. Halbhuber, Cell. Mol. Biol. **42,** 1181 (1996).
14. H. Oehring, I. Riemann, P. Fischer, K.-J. Halbhuber, and K. König, Scanning **22,** 263 (2000).
15. Y. Sako, A. Sekihata, Y. Yanagisawa, M. Yamamoto, Y. Shimada, K. Ozaki, and A. Kusumi, J. Microsc. **185,** 9 (1997).